

Reprinted from the Proceedings of the 1978 Symposium on the Effect of the Ionosphere on Space and Terrestrial Systems, Washington DC, 24-26 January 1978, sponsored by NRL/ONR.

## CHARGED-AREA EFFECTS ON SPACECRAFT DIELECTRIC ARC DISCHARGES

K.G. Balmain, P.C. Kremer and M. Cuchanski  
Department of Electrical Engineering  
University of Toronto  
Toronto, Canada M5S 1A4

### INTRODUCTION

A great quantity of evidence exists in support of the postulate that magnetic-substorm electrons cause arc discharges to occur on synchronous-orbit spacecraft [De Forest, 1972; Fredricks and Scarf, 1973; Rosen, 1975, 1976a, 1976b, 1976c]. Extensive laboratory simulation studies [Adamo and Nanevich, 1976; Balmain, 1973; Balmain, Orszag and Kremer, 1976; Hoffmaster and Sellen, 1976; Stevens, Lovell and Gore, 1976] have demonstrated the existence of strong and sometimes destructive arc discharges. These range from tiny micro-discharges on dielectric specimens exposed to the focussed beam of a scanning electron microscope, to destructive lightning-like arcs up to 30cm in length traversing the surface of large, thin sheets of metal-backed dielectric. The only existing theory of the arc breakdown has been put forward by Meulenber [1976], a theory which has become widely accepted and which describes the breakdown between a buried layer of impacted electrons and the electron-depleted surface of the material. Because this theory is one-dimensional, its applicability is primarily to the initial breakdown, while the propagation of the breakdown across the dielectric sheet very likely proceeds in the manner described by Gross [1957, 1958].

The main effect of discharge propagation apparently is to mobilize a large fraction of the available embedded-electron charge into a single arc which emits a burst of electrons with an accompanying downward pulse of current into the metal backing. Therefore, it might seem reasonable to expect that the dielectric specimen surface area would control the peak pulse current. The experiments to be described involve variations in surface area at two very different scales, one with specimens of varying area (of the order of  $1\text{cm}^2$ ) exposed to a fixed flood beam of electrons, and the other with varying electron beam cross-sectional areas (of the order of  $10^{-4}\text{cm}^2$ ) incident on specimens with much larger areas.

### MACRO-DISCHARGES

Large-scale dielectric specimens were mounted in a scanning electron microscope (SEM) which had been modified to produce an approximately uniform flood beam up to 10cm in diameter. In the experiments to be described, the accelerating voltage was 20kV and the beam current density was 1 to 2  $\mu\text{A}/\text{cm}^2$  incident on the dielectric surface. Shown in Fig. 1 is the experimental apparatus, including a 250 MHz bandwidth oscilloscope for display of the discharge current pulse.

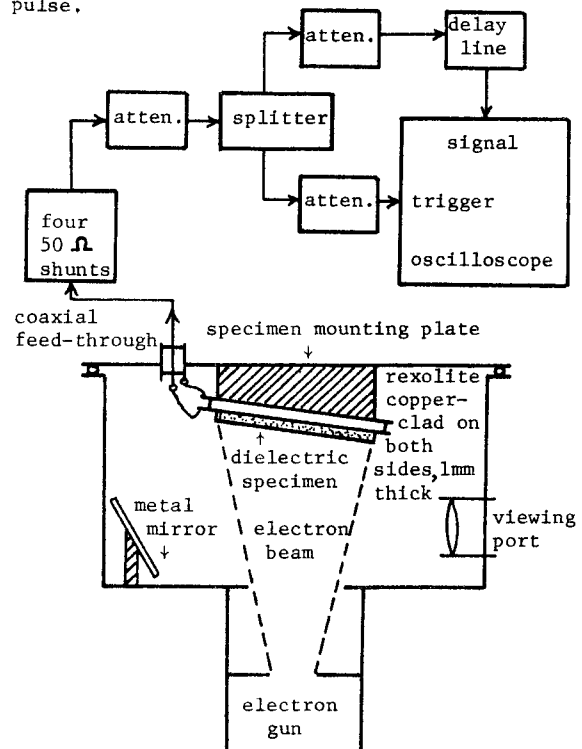
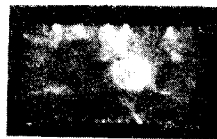


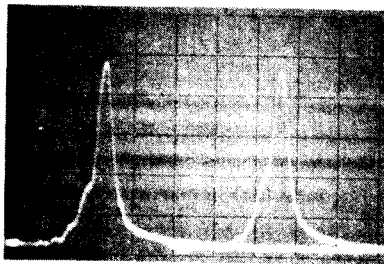
Fig. 1 The discharge current measurement system using the flood-beam mode in a modified SEM.



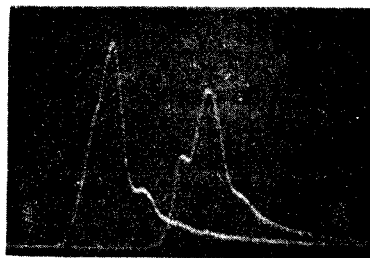
(a) Mylar specimen 48x26x0.12 mm, showing central illuminated region and arc going to lower edge.



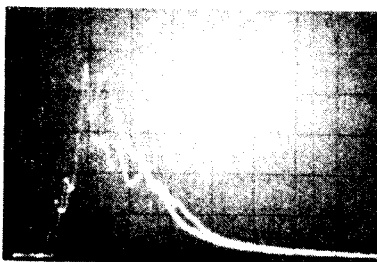
(b) Same specimen as at left, showing arc traversing illuminated region and going to upper edge.



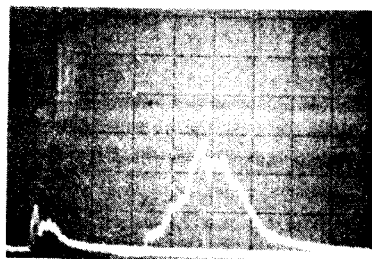
(c) 100 A peak current pulses on a 10 cm<sup>2</sup> Mylar specimen 0.1 mm thick. Hor. scale 50 ns/div.



(d) Quartz fabric discharges of 1.6 A and 1.3 A peak on a specimen of 2 cm<sup>2</sup>. Hor. scale 50 ns/div.



(e) Silvered-Teflon discharges of 20 A peak on a specimen of 10 cm<sup>2</sup>. Hor. scale 50 ns/div.



(f) Aluminized-Kapton discharges on a 5 cm<sup>2</sup> specimen, at 100 ns/div. Large pulse: 9 A peak.

Fig. 2 Examples of macro-discharges on various materials, for an incident-beam accelerating voltage of 20 kV.

A typical discharge arc can be seen in Fig. 2(a) as a "lightning stroke" extending from the central region to the lower edge of the specimen. The other rays extending outward to the edges are not arcs but rather luminescent streaks which appear for a short period after each discharge, when the reduced negative surface charge permits the incident electrons to reach the dielectric surface with appreciable energy. The central bright spot is illumination from the filament of the electron gun. In Fig. 2(b) an arc can be seen crossing the bright spot, thus indicating that the filament illumination is not strong enough to discharge the specimen by photoemission.

The strongest discharge currents measured

to date, 100 A peak, are shown in Fig. 2(c). Also shown in Fig. 2(d), (e) and (f) are typical discharges on quartz fabric, silvered-Teflon second-surface mirror, and aluminized-Kapton thermal blanket outer layer.

One silvered-Teflon specimen (not shown) had its central region covered with an electrically conductive material. This produced the unexpected result of increased complexity in appearance of the discharge arc, together with the occurrence of multiple-peaked current pulses.

In order to study the anticipated specimen-area effects, experiments were conducted in which a specimen was sequentially halved in area,

at each step being exposed to the flood beam of electrons. For each step at least six discharge current pulses were recorded and their peak currents averaged. The silvered-Teflon result of Fig. 3(a) for the first run (in which the specimens were alternately square and rectangular) suggests the existence of a definite power-law relationship between peak current and area. A second run (square specimens only) was not significantly different.

Similar experiments on copper-clad Mylar revealed the possibility of thickness dependence. Fig. 3(b) shows that the thicker specimen exhibits by far the greater discharge current. The reasons for this are not clear although conceivably they could involve occasional electron beam penetration of the thin specimen.

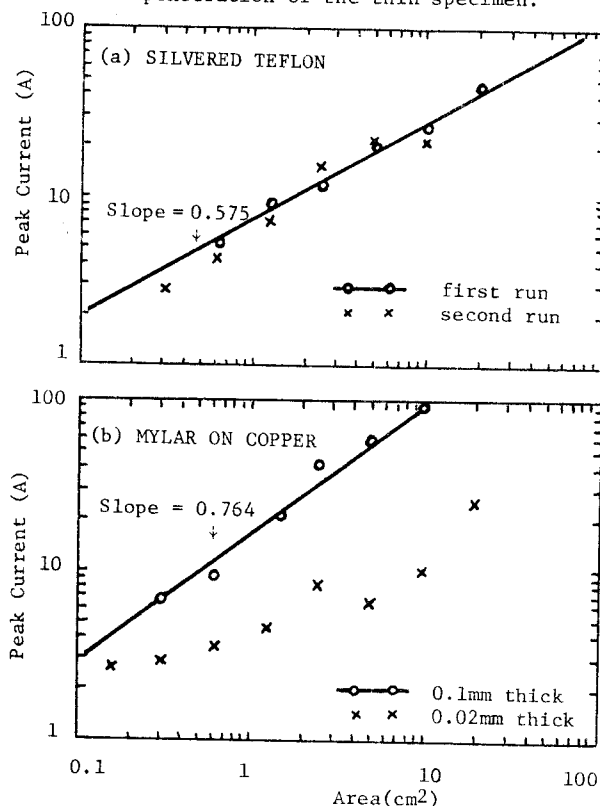


Fig. 3 The scaling of discharge peak current with specimen area for a 20kV beam.

It was observed that the discharge pulse duration is not simply related to the area. In the silvered-Teflon experiments the pulse duration (at half peak current) increased very erratically from 15ns to 100ns with increasing area. However, for the 0.1mm Mylar, the duration increased from 15ns to 25ns, again erratically. It is difficult to draw conclusions from these pulse duration observations although it can be said that the dielectric arcs bear little resemblance to capacitor discharges.

## MICRO-DISCHARGES

Defocusing of a stationary (non-scanned) electron beam in an SEM was found to be an effective means of charging a very small, measurable area on a dielectric specimen. Measurement of the beam diameter was achieved by using the beam to implant a "stripe" of electrons across the specimen. A secondary-electron image of the charged stripe was made by using the photographic scan mode of the SEM and examining the specimen after a brief exposure to air in order to neutralize excess surface charge. Knowing the magnification, it was straightforward to measure the stripe width and hence the beam diameter.

The micro-discharge current pulses were measured using a sampling oscilloscope with a 4GHz bandwidth, as shown in Fig. 4. A careful

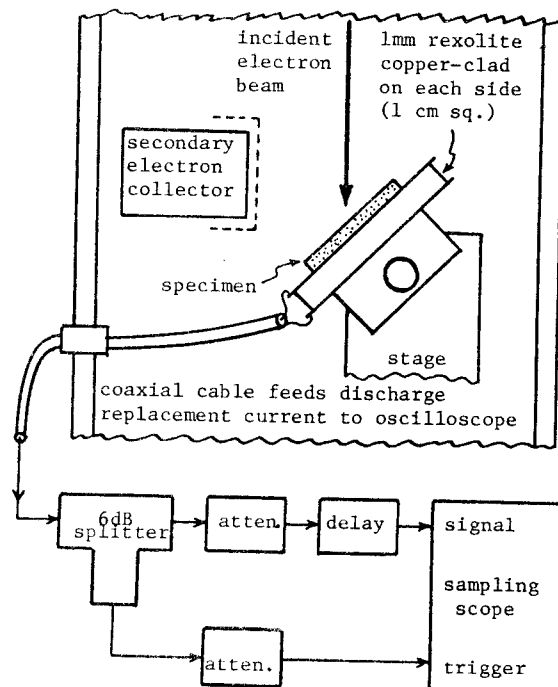


Fig. 4 Arrangement of components in specimen vacuum chamber of scanning electron microscope, and instrumentation for measuring micro-discharge current pulses.

setting of the oscilloscope trigger threshold made possible the selection of the strongest pulses, and the frequent discharge occurrence made possible the recording of relatively smooth pulse envelopes (an example of which is shown in Fig. 5) by taking one sample per pulse and stepping the sampling time through the duration of the pulse. The smoothness of the measured pulses indicates that the discharge phenomenon is highly repeatable within a small region of the dielectric surface. During each experiment the

discharge  
waveform

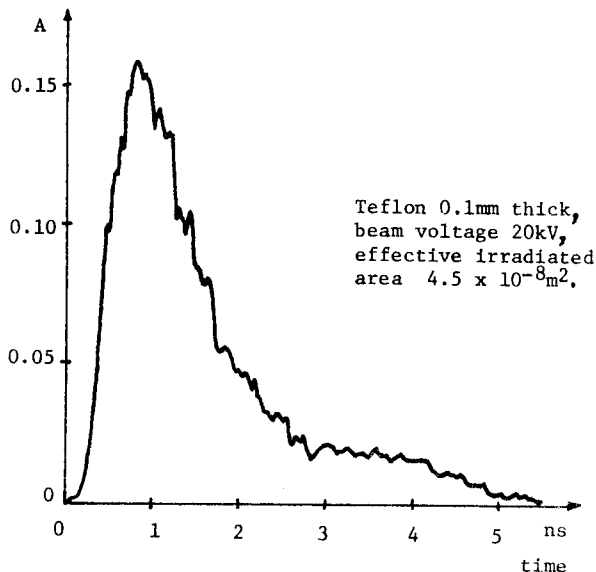


Fig. 5 A sampled current-pulse envelope.

position of the beam was changed very slowly to avoid "fatiguing" any point on the specimen.

Because of the slow beam movement described above, the effective charged area was estimated to be larger than the beam cross-section, and the area was computed as shown in Fig. 6.

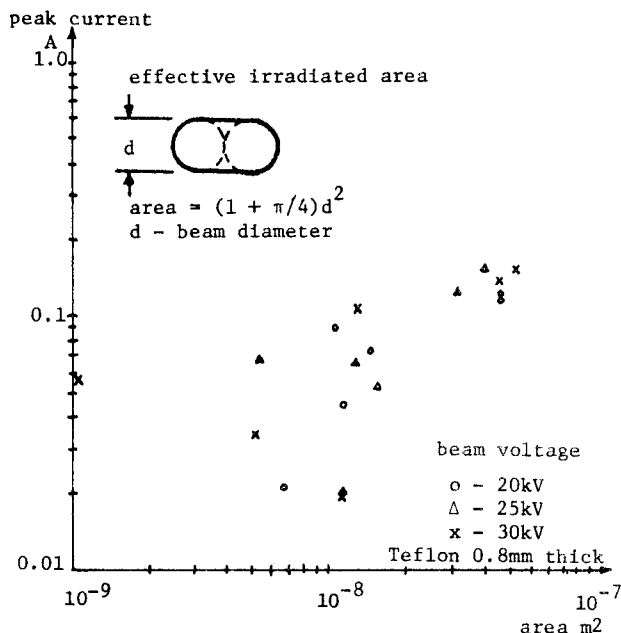


Fig. 6 Micro-discharge peak current as a function of charged area, with beam voltage as a parameter.

In the figure the experimental points show a definite tendency for peak current to increase with charged area, but the points exhibit no well-defined dependence on beam voltage. If beam voltage effects exist, they are not so pronounced as charged-area effects or the effects of using different materials such as Mylar, as indicated in Fig. 7.

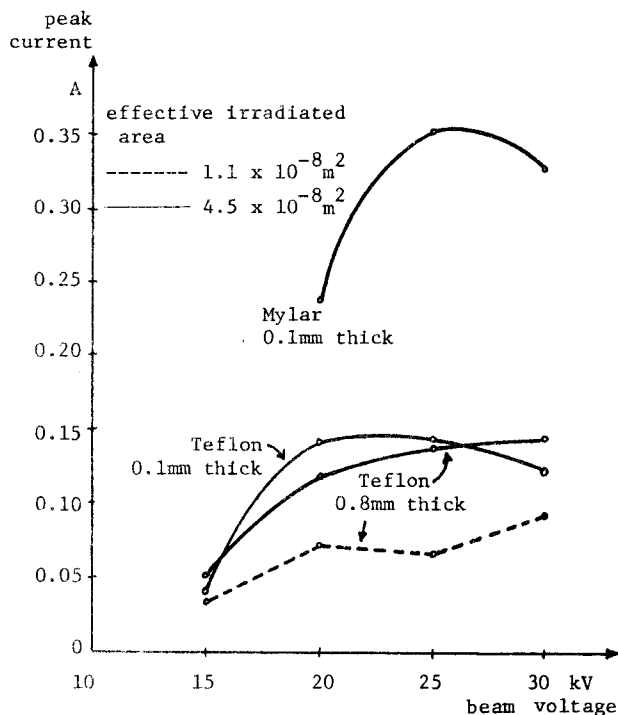


Fig. 7 Micro-discharge peak current dependence on material, specimen thickness, charged area and beam voltage.

The frequency of occurrence of discharge pulses is strongly dependent on beam voltage, as shown in Fig. 8. The low frequency of occurrence with Mylar is offset by high peak discharge currents, in terms of its potential as a source of electromagnetic interference.

The variations in pulse shape are summarized in Figs. 9 and 10, in terms of rise time and pulse width. Rise time is defined as the time interval between the 10% and 90% points, and pulse width is defined as the time interval between points at 1/3 the peak value. The rise time appears to increase with beam voltage, independent of area, while the pulse width shows a tendency to increase with area. Otherwise it is clear that pulse shape is characterized mainly by a high degree of variability.

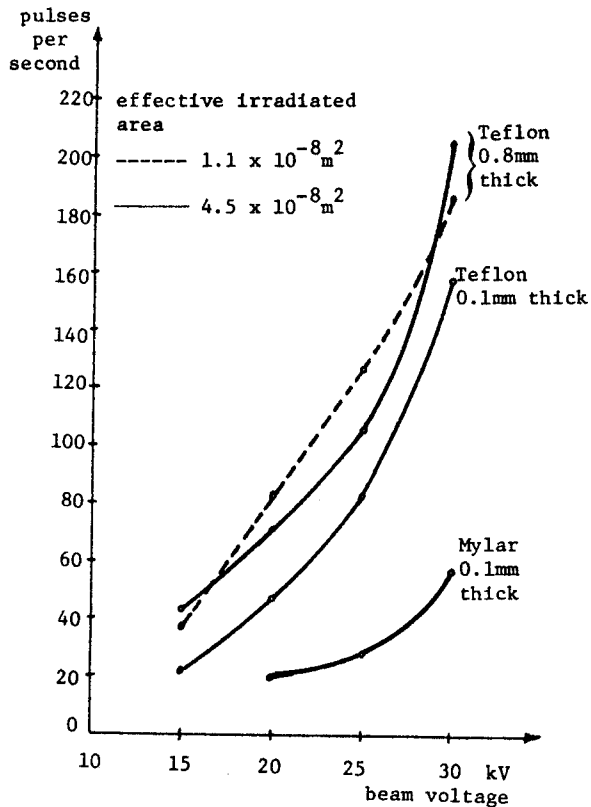


Fig. 8 Micro-discharge frequency of occurrence.

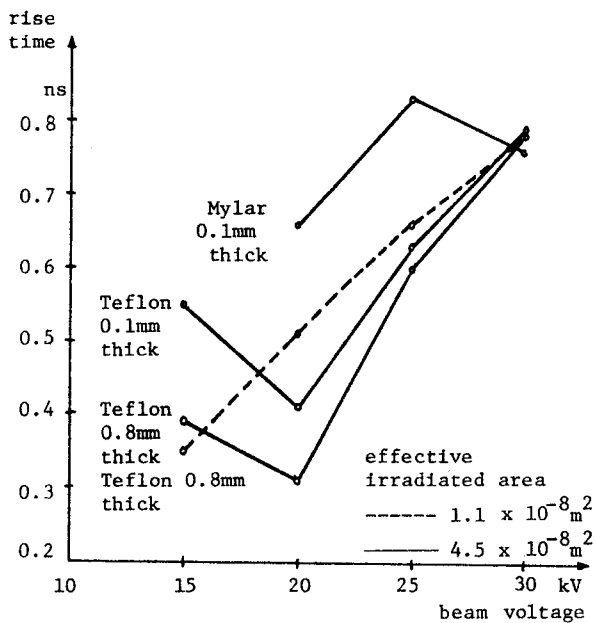


Fig. 9a Micro-discharge current pulse average rise time.

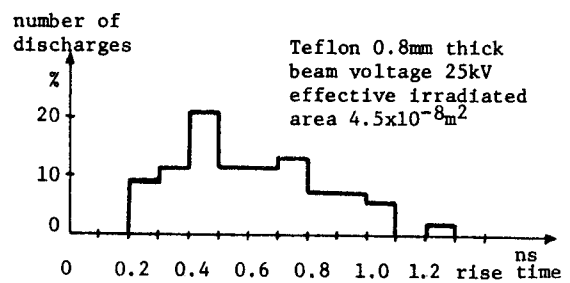


Fig. 9b Typical rise time histogram, calculated from 57 pulse envelopes.

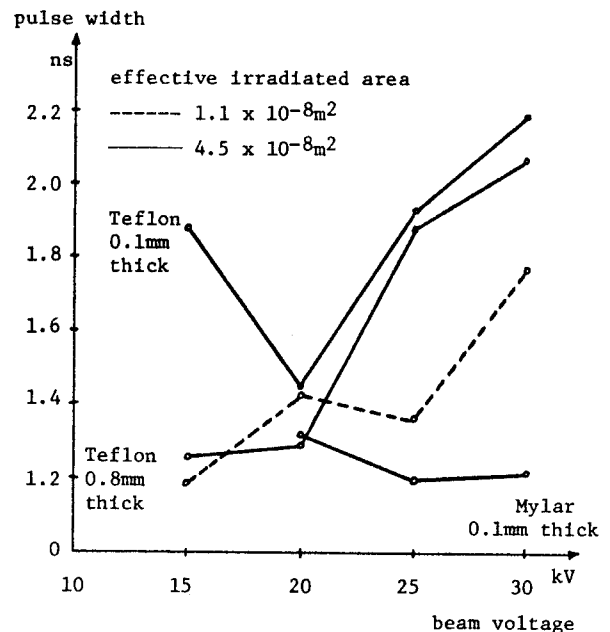


Fig. 10a Micro-discharge average pulse width.

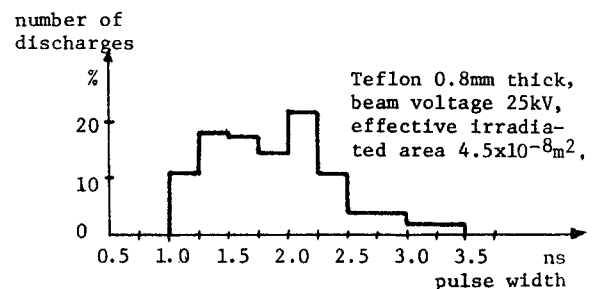


Fig. 10b Typical pulse width histogram, calculated from 57 pulse envelopes.

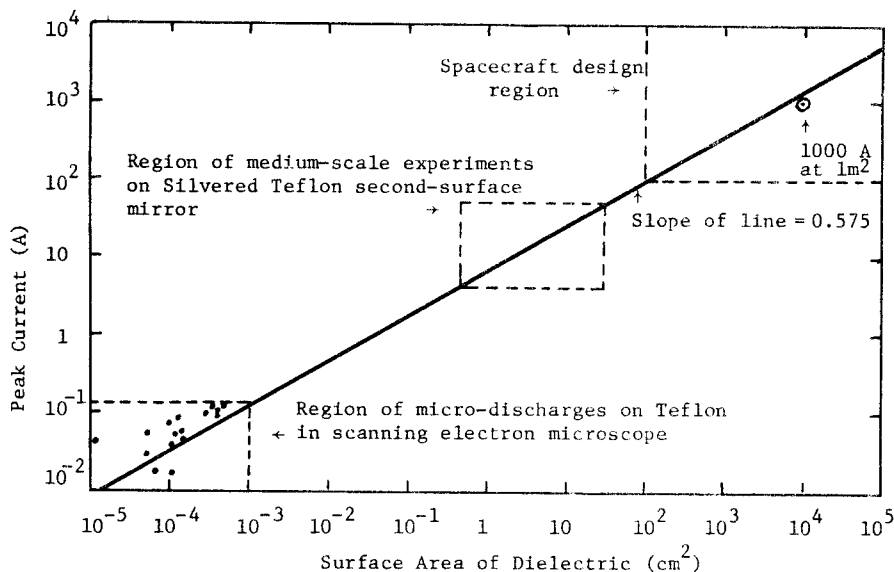


Fig. 11 Extrapolation of macro-discharge peak-current scaling law for Teflon (from Fig. 3a). The dots indicate micro-discharge data for Teflon (from Fig. 6, without distinction as to beam voltage).

#### CONCLUSIONS

A definite tendency for discharge peak current to increase with increasing charged area has been identified for both macro-discharges and micro-discharges. The experimental data from both regimes is plotted on the same graph in Fig. 11, in which the extrapolated macro-discharge straight-line characteristic can be seen to pass close to the micro-discharge experimental points. The fit of this line to the micro-discharge points would be very close if the effective charged area were larger by a factor of about two, a realistic possibility. The existence of this simple power-law relationship between current and area is the first concrete evidence that macro-discharges and micro-discharges are just different orders of magnitude of the same basic phenomenon.

Because there is no indication of flattening out of the current-versus-area characteristic, extrapolation to larger effective charged areas may be justified. The extrapolated characteristic of Fig. 11 passes above 1000 A at  $1\text{ m}^2$ , suggestive of extremely strong electromagnetic interference effects for spacecraft-size metal-backed dielectric sheets.

For Mylar the existence of a simple current-versus-area scaling characteristic appears much less certain. Within the ranges of parameters tested, compared to Teflon, Mylar exhibits less frequent but stronger discharges.

In general, it can be concluded that standard and modified scanning electron microscopes can provide discharge data over very wide ranges of parameters. Therefore, larger and more expensive vacuum chambers appear to be unnecessary for much of the experimentation necessary to gain an understanding of surface discharge arcs and to develop new and better spacecraft materials.

#### ACKNOWLEDGMENTS

The authors acknowledge with pleasure the contributions of M. Palfreyman, J.V. Gore, W.L. Lehn and W.C. Nixon. The research was supported by the Communications Research Centre, Department of Communications, Canada, under Department of Supply and Services Contract No. OSU 76-00064. Permission by the Department of Communications to publish the results of this study is acknowledged. Support was also provided by the National Research Council of Canada, under Grant No. A-4140.

#### REFERENCES

- Adamo, R.C. and J.E. Nanevich (1976), Spacecraft-charging studies of voltage breakdown processes on spacecraft thermal control mirrors, in Spacecraft Charging by Magnetospheric Plasmas, A. Rosen (Ed.), Progress in Astronautics and Aeronautics, 47, 225-235.

- Balmain, K.G. (1973), Charging of spacecraft materials simulated in a scanning electron microscope, Electronics Letters, 9, No. 23 544-546.
- Balmain, K.G., M. Orszag, and P. Kremer (1976), Surface discharges on spacecraft dielectrics in a scanning electron microscope, in Spacecraft Charging by Magnetospheric Plasmas, A. Rosen (Ed.), Progress in Astronautics and Aeronautics, 47, 213-223.
- De Forest, S.E. (1972), Spacecraft charging at synchronous orbit, J. Geophys. Res., 77, 651-659.
- Fredricks, R.W., and Scarf, F.L. (1973), Observations of spacecraft charging effects in energetic plasma regions, in Photon and Particle Interactions with Surfaces in Space, Reidel, Dordrecht-Holland, 277-308.
- Gross, B. (1957), Irradiation effects in borosilicate glass, Phys. Rev., 107, 368-373.
- Gross, B. (1958), Irradiation effects in Plexiglas, J. Polymer Sci., 27, 135-143.
- Hoffmaster, D.K. and J.M. Sellen Jr. (1976), Spacecraft material response to geosynchronous substorm conditions, in Spacecraft Charging in Magnetospheric Plasmas, A. Rosen (Ed.), Progress in Astronautics and Aeronautics, 47, 185-211.
- Meulenberg, A., Jr. (1976), Evidence for a new discharge mechanism for dielectrics in a plasma, in Spacecraft Charging by Magnetospheric Plasmas, A. Rosen (Ed.), Progress in Astronautics and Aeronautics, 47, 237-246.
- Rosen, A. (1975), Large discharges and arcs on spacecraft, Astronautics and Aeronautics, June, 36-44.
- Rosen, A. (1976 a), Spacecraft charging: Environment-induced anomalies, J. Spacecraft and Rockets, 13, 129-136.
- Rosen, A., Ed. (1976 b), Spacecraft Charging by Magnetospheric Plasmas, Progress in Astronautics and Aeronautics, 47.
- Rosen, A. (1976 c), Spacecraft charging by magnetospheric plasmas, IEEE Transactions on Nuclear Science, NS-23, 1762-1768.
- Stevens, N.J., R.R. Lovell, and J.V. Gore (1976), Spacecraft-charging investigation for the CTS project, in Spacecraft Charging by Magnetospheric Plasmas, A. Rosen (Ed.), Progress in Astronautics and Aeronautics, 47, 263-275.